NeuroImage: Clinical 38 (2023) 103445

Contents lists available at ScienceDirect

NeuroImage: Clinical

journal homepage: www.elsevier.com/locate/ynicl

Frequency-dependent and time-variant alterations of neural activity in post-stroke depression: A resting-state fMRI study

Xiumei Wu [a,b,1], Luoyu Wang [a,c,1], Haibo Jiang [d], Yanhui Fu [e], Tiantian Wang [a,b], Zhenqiang Ma [e], Xiaoyan Wu [f], Yiying Wang [g], Fengmei Fan [h,*], Yulin Song [e,*], Yating Lv [a,b,*]

[a] Center for Cognition and Brain Disorders, The Affiliated Hospital of Hangzhou Normal University, Hangzhou, Zhejiang, China
[b] Zhejiang Key Laboratory for Research in Assessment of Cognitive Impairments, Hangzhou, Zhejiang, China
[c] Department of Radiology, Affiliated Hangzhou First People's Hospital, Zhejiang University School of Medicine, Hangzhou, Zhejiang, China
[d] Department of Neurology, The Affiliated Hospital of Hangzhou Normal University, Hangzhou, Zhejiang, China
[e] Department of Neurology, Anshan Changda Hospital, Anshan, Liaoning, China
[f] Department of Image, Anshan Changda Hospital, Anshan, Liaoning, China
[g] Department of Ultrasonics, Anshan Changda Hospital, Anshan, Liaoning, China
[h] Beijing Huilongguan Hospital, Peking University Huilongguan Clinical Medical School, Beijing, China

ARTICLE INFO

Keywords:
Post-stroke depression
Resting-state functional magnetic resonance imaging
Amplitude of low-frequency fluctuation
Frequency bands
Temporal dynamics

ABSTRACT

Background: Post-stroke depression (PSD) is one of the most frequent psychiatric disorders after stroke. However, the underlying brain mechanism of PSD remains unclarified. Using the amplitude of low-frequency fluctuation (ALFF) approach, we aimed to investigate the abnormalities of neural activity in PSD patients, and further explored the frequency and time properties of ALFF changes in PSD.

Methods: Resting-state fMRI data and clinical data were collected from 39 PSD patients (PSD), 82 S patients without depression (Stroke), and 74 age- and sex-matched healthy controls (HC). ALFF across three frequency bands (ALFF-Classic: 0.01–0.08 Hz; ALFF-Slow4: 0.027–0.073 Hz; ALFF-Slow5: 0.01–0.027 Hz) and dynamic ALFF (dALFF) were computed and compared among three groups. Ridge regression analyses and spearman's correlation analyses were further applied to explore the relationship between PSD-specific alterations and depression severity in PSD.

Results: We found that PSD-specific alterations of ALFF were frequency-dependent and time-variant. Specially, compared to both Stroke and HC groups, PSD exhibited increased ALFF in the contralesional dorsolateral prefrontal cortex (DLPFC) and insula in all three frequency bands. Increased ALFF in ipsilesional DLPFC were observed in both slow-4 and classic frequency bands which were positively correlated with depression scales in PSD, while increased ALFF in the bilateral hippocampus and contralesional rolandic operculum were only found in slow-5 frequency band. These PSD-specific alterations in different frequency bands could predict depression severity. Moreover, decreased dALFF in contralesional superior temporal gyrus were observed in PSD group.

Limitations: Longitudinal studies are required to explore the alterations of ALFF in PSD as the disease progress.

Conclusions: The frequency-dependent and time-variant properties of ALFF could reflect the PSD-specific alterations in complementary ways, which may assist to elucidate underlying neural mechanisms and be helpful for early diagnosis and interventions for the disease.

1. Introduction

Post-stroke depression (PSD) is one of the most frequent psychiatric disorders after stroke (Loubinoux et al., 2012), affecting approximately one-third of stroke survivors (Ayerbe et al., 2013; Hackett and Pickles, 2014). It has been reported that depression after stroke is linked with

* Corresponding authors at: Centre for Cognition and Brain Disorders, The Affiliated Hospital of Hangzhou Normal University, Hangzhou 310015, China (Y. Lv). Department of Neurology, Anshan Changda Hospital, Anshan, Liaoning 114005, China (Y. Song). Beijing Huilongguan Hospital, Peking University Huilongguan Clinical Medical School, Beijing 100096, China (F. Fan).
E-mail addresses: fanfengmei@live.com (F. Fan), yulinsong1969@sina.com (Y. Song), lvyating198247@gmail.com (Y. Lv).
[1] These authors contributed equally, they share the first authorship.

https://doi.org/10.1016/j.nicl.2023.103445
Received 10 April 2023; Received in revised form 23 May 2023; Accepted 24 May 2023
Available online 29 May 2023

lower quality of life, poor functional prognosis and higher mortality (Ayerbe et al., 2013; Cai et al., 2019; Robinson and Jorge, 2016; Wijeratne and Sales, 2021). However, the underlying brain mechanism of PSD remains unclarified (Loubinoux et al., 2012). Therefore, it is necessary to identify the functional brain abnormalities in PSD patients, which may help to elucidate neural mechanisms and be useful for early diagnosis and developing specific therapeutic interventions for the disease (Robinson and Jorge, 2016).

Resting-state functional magnetic resonance imaging (rs-fMRI), which measures spontaneous neuronal activity, is a promising tool to investigate brain abnormalities in various brain disorders without completing any task (Fox and Raichle, 2007; Fu et al., 2018; Veldsman et al., 2015). Using resting-state functional connectivity approach, previous studies reflected that PSD is associated with impaired interregional connectivity within default mode network, central executive network, affective network, cognitive control network and so on (Balaev et al., 2018; Liang et al., 2020; Shi et al., 2017; Zhang et al., 2018; Zhang et al., 2014; Zhang et al., 2019). However, connectivity-based approaches only assess the synchronization patterns of the spontaneous brain activity between regions (Fox and Greicius, 2010), cannot reveal the local neural activity changes in specific brain regions. Amplitude of low-frequency fluctuation (ALFF), which calculated by the mean amplitude of blood oxygenation level dependent (BOLD) signal within low frequency range, has been proposed to directly measure the intensity of local neural activity (Zang et al., 2007). The ALFF has been widely applied to localize the functional abnormalities in brain disorders (Bu et al., 2019; Cui et al., 2020; Hare et al., 2017; Li et al., 2019; Skidmore et al., 2013). With respect to PSD, however, few studies have been conducted to evaluate from the perspective of alterations in regional spontaneous neuronal activity. Two recent studies employed the fractional ALFF (fALFF) approach and observed that PSD patients showed increased fALFF in the left dorsolateral prefrontal cortex and the right precentral gyrus (Egorova et al., 2017), and PSD-related alterations of fALFF were associated with the severity of depression (Goodin et al., 2019). However, these two studies only recruited stroke patients (i.e., non-PSD vs. PSD; Low depressive symptom score group vs. High depressive symptom score group), and did not rule out the possible effect of the lesions on their results during data processing, thus the relevant findings need further validation under consideration of healthy controls and with the lesions excluded in patients.

In addition, previous studies have examined ALFF at more refined frequencies and showed that the alterations of ALFF exhibited frequency-dependent patterns in patients with stroke and major depressive disorder (MDD) (Chang et al., 2019; Goodin et al., 2019; Quan et al., 2022; Wang et al., 2016; Wu et al., 2020a; Zuo et al., 2010). For example, Wang and colleagues indicated that ALFF in slow-5 frequency band (0.01–0.027 Hz) was more sensitive to local functional abnormalities in the left ventromedial prefrontal cortex, left precentral gyrus and bilateral posterior cingulate cortex than slow-4 frequency band (0.027–0.073 Hz) in MDD (Wang et al., 2016). On the other hand, the neuronal activity is highly dynamic and fluctuates over time even at rest (Allen et al., 2014; Fu et al., 2018; Guo et al., 2019; Smith et al., 2012). Traditional resting-state fMRI metrics, such as functional connectivity and ALFF, are usually calculated over the entire duration of the resting-state fMRI session, which may overlook the valuable information within the temporal features of neural fluctuations (Allen et al., 2014; Hutchison et al., 2013; Smith et al., 2012; Wang et al., 2019). Whereas dynamic ALFF (dALFF), calculating the standard deviation or variability of the traditional static ALFF in all windows by sliding window approach, is a stable metric to capture the temporal variability of regional neural activity (Fu et al., 2018; Liao et al., 2019; Yan et al., 2017). At present, dALFF has been applied to explore the functional abnormalities and improve the classification accuracy in brain disorders, including depression (Li et al., 2019), schizophrenia (Fu et al., 2018), generalized anxiety disorder (Cui et al., 2020), poststroke aphasia (Guo et al., 2019), indicating that dALFF could serve as a complementary measure to static ALFF. Therefore, the frequency-dependent pattern and temporal variability of ALFF should be also examined to provide a more complete view of local disruptions in PSD.

In the current study, we employed resting-state fMRI to investigate the alterations of spontaneous neural activity in patients with PSD. Specifically, we sought to identify the alterations of ALFF in different frequency bands and determine the temporal variability of ALFF in PSD patients as compared to nondepressed stroke patients and healthy controls. For the PSD-specific alterations of ALFF, we further explored their associations with depression severity in PSD patients.

2. Materials and methods

2.1. Participants

One hundred and twenty-seven patients who had first time ischemic stroke were recruited from the Department of Neurology, Anshan Changda Hospital from April 2018 to June 2021, including 88 S patients without depression (Stroke group, 33 females) and 39 post-stroke depression patients (PSD group, 18 females). Seventy-four age- and sex-matched healthy controls (HC group, 31 females) were also enrolled from the local community. All the participants were right-handed. The Ethics Committee of the Center for Cognition and Brain Disorders, Hangzhou Normal University approved this study, and each participant signed an informed consent.

Each patient met the following inclusion criteria: (a) diagnosis of ischemic stroke by neurologists; (b) admitted $<$ 1 month after stroke onset; (c) unilateral focal brain lesions. Patients were excluded if they had other psychiatric disease history, hemorrhage, leukoaraiosis, epilepsy or migraine. PSD patients were diagnosed by professional neurologists, in conformity with the Diagnostic Statistical Manual of Mental Disorder, Fifth Edition (DSM-V) criteria. All enrolled patients did not take any antidepressants before MRI scanning. Healthy controls were enrolled when they had no history of physical or psychiatric diseases.

2.2. Data acquisition

2.2.1. Clinical assessments

Within 24 h before the MRI scanning, participants completed the following assessments: National Institutes of Health Stroke Scale (NIHSS), Activity Daily Living Scale (ADL), Self-Rating Anxiety Scale (SAS), Hamilton Depression Rating Scale (HAMD), Patient Health Questionnaire-9 (PHQ-9) and Center for Epidemiological Survey Depression Scale (CES-D). Additionally, the risk factors of patients including diabetes, hypertension, smoking, alcohol, and dyslipidemia were recorded as well.

2.2.2. Multimodal MRI data acquisition

Each patient underwent MRI scanning within one month after stroke onset. During the scan, all participants were instructed to close their eyes, stay awake and hold still. The MRI scanning protocol for this study included rs-fMRI, structural MRI (sMRI) and diffusion-weighted imaging (DWI). The MRI data were collected on a 3-Tesla scanner (GE MR-750, Waukesha, WI) at Anshan Changda Hospital with the following parameters: (1) rs-fMRI: acquired with an echo-planar imaging sequence, axial slice = 43, slice thickness/gap = 3.2/0 mm, echo time (TE) = 30 ms, repetition time (TR) = 2000 ms, field of view (FOV) = 220 × 220 mm^2, matrix size = 64 × 64, voxel size = 3.4 mm × 3.4 mm × 3.2 mm, flip angle (FA) = 90°, volumes = 240, time = 8′, and parallel acceleration = 2; (2) sMRI: acquired using a 3D-MPRAGE sequence, sagittal slice = 176, slice thickness/gap = 1/0 mm, TE = 3.1 ms, TR = 8100 ms, FOV = 256 × 256 mm^2, matrix size = 256 × 256, voxel size = 1 mm × 1 mm × 1 mm, FA = 8°, time = 5′05″, prepare time = 450 ms, bandwidth = 31.25 kHz and parallel acceleration = 2; (3) DWI: axial slice = 22, slice thickness/gap = 5/1 mm, TR = 4000 ms, FOV = 240 × 240 mm^2, b = 1000, time = 1′.

2.3. Data preprocessing

2.3.1. Processing of sMRI image and lesion map

Using ITK-SNAP software (https://www.itksnap.org), one radiologist (F.C. with 5 years of experience), blinded to clinical information of the patients, manually traced lesion masks based on high-resolution sMRI and DWI images for each patient. The masks were smoothed with 3 mm full-width half maximum (FWHM) to remove jagged edges created during the drawing (Rorden et al., 2012). For patients whose lesion on the right hemisphere, the lesion masks, DWI and sMRI images were flipped from right to left. Subsequently, due to the distortion of lesion for the segmentation and normalization of the sMRI image, the abnormal values within the lesion were replaced with values in the contralesional homologous regions using clinicaltbx (https://www.nitrc.org/plugins/mwiki/index.php/clinicaltbx:MainPage) based on Statistical Parametric Mapping (SPM) (Nachev et al., 2008). The corrected sMRI images were then segmented and normalized to the Montreal Neurological Institute (MNI) space to obtain deformation information. For each patient, the two lesion masks from sMRI and DWI images were further normalized to the MNI space via deformation fields derived from tissue segmentation of sMRI images. We then calculated the union of two masks to obtain the lesion map for each patient. Fig. 1 displays the overlap of the lesion maps for Stroke patients and PSD patients, respectively.

2.3.2. Preprocessing of resting-state fMRI data

The rs-fMRI data preprocessing was performed in SPM12 (https://www.fil.ion.ucl.ac.uk/spm) and Data Processing & Analysis for Brain Imaging (DPABI, https://rfmri.org/dpabi) (Yan et al., 2016). Preprocessing steps included: 1) The lesion side was uniformly set to the left side, for patients with lesions located on the right hemisphere, the fMRI data were flipped from right to left around the mid-sagittal line (Allman et al., 2016; Bestmann et al., 2010; Schaechter et al., 2009); 2) removal of the first 10 volumes; 3) correction for intra-volume time delays between slices via Sinc interpolation; 4) correction for inter-volume head motion based on rigid-body transformation; 5) spatial normalization to the MNI space by deformation fields derived from tissue segmentation of sMRI images as described above; 6) spatial smoothing with an isotropic Gaussian kernel of 6 mm full width at half maximum (FWHM); 7) removal of linear trends; 8) making individual white matter (WM) and cerebrospinal fluid (CSF) masks: 95% probability masks of individual WM and CSF obtained from segmentation of sMRI image were first normalized to MNI space for each participant. The normalized masks were first intersected with WM and CSF template in DPABI, and then removed the lesion for each patient to obtain individual WM mask and CSF mask; 9) regressing out nuisance signals including 24-parameter head motion profiles (Friston et al., 1996), individual WM signal and CSF signal (the average time series extracted from individual WM mask and CSF mask). We did not regress out the global signals as this step is controversial for rs-fMRI data (Murphy and Fox, 2017); 10) making gray matter mask for all participants: the smoothed fMRI data were used to extract the whole brain mask by the function 'w_Automask' in DPABI. The intersection of all brain masks was further intersected with the Anatomical Automatic Labeling (AAL) atlas with 8 subcortical regions (thalamus and basal ganglia) and white matter removed to obtain gray matter mask; 11) removing the effects of hemodynamic lags: to correct hemodynamic lags for each patient in Stroke and PSD groups, we shifted the time series of each voxel according to their hemodynamic lags as calculated by time-shift analysis approach proposed in our previous study using the average time series of the gray matter mask as reference time series (Lv et al., 2013). The shifted time series were then used for ALFF calculation.

Notably, six participants in Stroke group who met the head movement criterion of maximal displacement > 3 mm, rotation $> 3°$ or mean framewise displacement (FD) > 0.5 were excluded (Power et al., 2012), leaving 82 patients in Stroke group (mean FD: 0.16 ± 0.10), 39 PSD patients (mean FD: 0.15 ± 0.07) and 74 HC (mean FD: 0.11 ± 0.07) in the following analyses.

2.4. ALFF calculation

2.4.1. Static ALFF

Static ALFF was calculated via the RESTplus software (https://restfmri.net/forum/RESTplus) (Jia et al., 2019). After preprocessing rs-fMRI data, we transformed the time series of each voxel to the frequency domain using Fast Fourier Transformation and acquired the power spectrum for each participant. And then we calculated the averaged square root of power spectrum in three frequency bands: 0.01–0.08 Hz (ALFF-Classic), 0.01–0.027 Hz (ALFF-Slow5) and 0.027–0.073 Hz (ALFF-Slow4). Each of these ALFF values was further divided by the individual whole-brain mean ALFF for standardization and subsequent statistical analyses (Zang et al., 2007; Zuo et al., 2010).

2.4.2. Dynamic ALFF

Dynamic ALFF was performed using Temporal Dynamic Analysis (TDA) toolkit based on RESTplus (https://restfmri.net/forum/

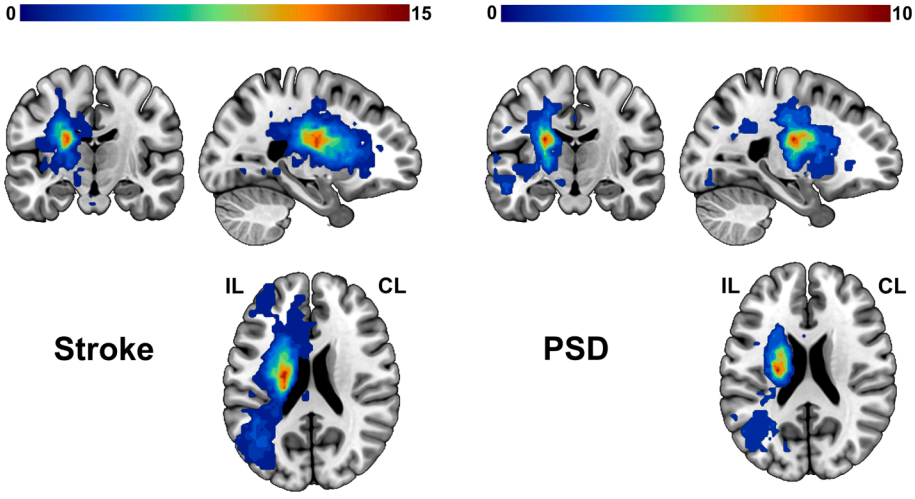

Fig. 1. Overlap maps of lesions. Lesions were overlapped in Stroke (left) and PSD group (right). The color depicts the number of patients with focal brain lesion at any given location. ***Abbreviations:*** Stroke, stroke patients without depression; PSD, post-stroke depression; IL, ipsilesional hemisphere; CL, contralesional hemisphere.

RESTplus) (Jia et al., 2019). The sliding window approach, which is sensitive to detect time-dependent variations of BOLD signal fluctuations, was adopted to calculate dALFF (Fu et al., 2018). We employed a sliding window length of 50 TR (100 s) and a step size of 1 TR (2 s) according to the rule of thumb for minimal window length which should be $>1/f_{min}$ (f_{min} is the minimum frequency of time series) (Leonardi and Van De Ville, 2015). For each participant, the ALFF (0.01–0.08 Hz) values of whole-brain voxels were calculated in each time window and a total of 181 ALFF maps were acquired during the sliding window process. We then calculated the standard deviation (dALFF-SD) and the corresponding coefficient of variation (dALFF-CV, dALFF-CV = dALFF-SD/mean) of each voxel for each participant to evaluate the temporal variability of dALFF.

2.5. Statistical analysis

2.5.1. Among-group differences in demographic and clinical data

For comparison of differences in demographic and clinical variables among three groups or between Stroke and PSD groups in SPSS26.0 (IBMCorp., Armonk, N.Y., USA), chi-square tests were used for categorical data (i.e., gender, lesion hemisphere), one-way analysis of variance (ANOVA) and two-sample *t*-test for continuous data (i.e., age, PHQ-9, NIHSS).

2.5.2. Among-group differences in ALFF

For five ALFF maps (ALFF-Classic, ALFF-Slow4, ALFF-Slow5, dALFF-SD and dALFF-CV) in Stroke, PSD and HC groups, one-way ANOVA analyses were conducted to compare the ALFF differences among three groups within the gray matter mask obtained from data preprocessing using DPABI (https://rfmri.org/dpabi) (Yan et al., 2016). The age and gender were treated as covariates of no interest. Voxel-level false discovery rate (FDR) procedure was applied to correct for multiple comparisons, with a threshold of $q < 0.05$ and cluster size > 20 voxels.

For any region showing significant differences in five ALFF metrics among three groups, post-hoc analyses were further performed to compare the average ALFF values in each region between each pair of groups in SPSS. The regions showing higher or lower ALFF values in PSD group than both Stroke and HC groups were identified as the PSD-specific alterations. The thresholds for post-hoc analyses were set as $p < 0.05$.

2.5.3. Ridge regression analysis

To clarify the relationship between the PSD-specific ALFF alterations and depression severity, we predicted the depression scale scores (HAMD, PHQ-9 and CES-D) for each participant in PSD group using ridge regression analysis based on the scikit-learn library in Python (https://scikit-learn.org/stable/). Briefly, the average ALFF values extracted from each of PSD-specific regions in PSD group were used as the features. Leave-One-Out Cross-Validation (LOO-CV) and grid search were applied to determine the optimal penalty coefficient, resulting in reliable ridge regression model for each depression scale. And we further conducted the correlation analyses using the predicted scores and the real scores obtained from the ridge regression models.

2.5.4. Correlation analysis

For each region showing PSD-specific alterations of each ALFF metric (ALFF-Classic, ALFF-Slow4, ALFF-Slow5, dALFF-SD and dALFF-CV), a Spearman's correlation analysis was performed between the average ALFF metric value in the region and each depression scale score (HAMD, PHQ-9 and CES-D) in PSD group. The significance of correlation analysis was defined as $p < 0.017$ ($p < 0.05/3$, Bonferroni corrected).

3. Results

3.1. Demographics and clinical characteristics

Demographic and clinical information for the final 82 S patients without depression (Stroke, 59.41 ± 6.45 years, 32 females), 39 PSD patients (PSD, 60.00 ± 9.41 years, 18 females) and 74 healthy controls (HC, 57.43 ± 6.83 years, 31 females) were presented in Table 1. There

Table 1
Demographic and clinical characteristics of participants.

	Stroke (n = 82)	PSD (n = 39)	HC (n = 74)	*p* value
Gender (M/F)	50/32	21/18	43/31	0.756[a]
Age (years)	59.41 ± 6.45	60.00 ± 9.41	57.43 ± 6.83	0.121[b]
Blood systolic pressure (mmHg)	163.68 ± 21.67[d]	173.13 ± 28.38[e]	129.10 ± 15.53[f]	< 0.001[b]
Blood diastolic pressure (mmHg)	92.58 ± 12.64[d]	91.89 ± 15.09[e]	81.32 ± 9.73[f]	< 0.001[b]
Blood sugar level (mmol/L)	7.59 ± 3.19[g]	7.35 ± 3.36[h]	5.32 ± 0.67[i]	< 0.001[b]
Total cholesterol (mmol/L)	5.34 ± 1.24[j]	4.62 ± 1.23[h]	5.02 ± 0.98[k]	< 0.010[b]
Smoking, No. (%)	36 (43.90%)	18 (46.15%)		0.816[a]
Drinking, No. (%)	43 (52.44%)[g]	24 (61.54%)[l]		0.230[a]
Onset time (days)	4.85 ± 3.26	9.92 ± 4.92		< 0.001[c]
Lesion hemisphere (L/R)	44/38	23/16		0.582[a]
Lesion size (voxels)	128.42 ± 256.28	128.94 ± 178.17		0.992[c]
PHQ-9	0.2 ± 0.7	8.2 ± 2.9	0.7 ± 1.2	< 0.001[b]
ADL	82.8 ± 16.8	67.1 ± 18.1	100 ± 0.0	< 0.001[b]
NIHSS	2.5 ± 2.2	5.2 ± 3.5		< 0.001[c]
SAS	25.1 ± 0.8	32.2 ± 5.0		< 0.001[c]
HAMD	0.2 ± 0.8	19.2 ± 2.0		< 0.001[c]
CES-D	12.1 ± 0.6	24.4 ± 4.4		< 0.001[c]

Abbreviations: Stroke, stroke patients without depression; PSD, post-stroke depression; HC, healthy controls; M, male; F, female; L, left; R, right; PHQ-9, Patient Health Questionnaire-9; ADL, Activity Daily Living Scale; NIHSS, National Institutes of Health Stroke Scale; SAS, Self-Rating Anxiety Scale; HAMD, Hamilton Depression Rating Scale; CES-D, Center for Epidemiological Survey Depression Scale.

Blood systolic pressure (mmHg) post-hoc *t*-tests: Stroke vs HC ($p < 0.001$); PSD vs HC ($p < 0.001$).

Blood diastolic pressure (mmHg) post-hoc *t*-tests: Stroke vs HC ($p < 0.001$); PSD vs HC ($p < 0.001$).

Blood sugar level (mmol/L) post-hoc *t*-tests: Stroke vs HC ($p < 0.001$); PSD vs HC ($p < 0.01$).

Total cholesterol (mmol/L) post-hoc *t*-tests: Stroke vs PSD ($p < 0.05$).

PHQ-9 post-hoc *t*-tests: PSD vs HC ($p < 0.001$); Stroke vs PSD ($p < 0.001$).

ADL post-hoc *t*-tests: Stroke vs HC ($p < 0.001$); PSD vs HC ($p < 0.001$); Stroke vs PSD ($p < 0.001$).

[a] The *p*-value was obtained by a chi-square test.
[b] The *p*-values were obtained by one-way analysis of variance tests.
[c] The *p*-values were obtained by two-sample *t*-tests.
[d] Data were missing for 2 participants in Stroke group.
[e] Data were missing for 1 participant in PSD group.
[f] Data were missing for 6 participants in HC group.
[g] Data were missing for 6 participants in Stroke group.
[h] Data were missing for 3 participants in PSD group.
[i] Data were missing for 10 participants in HC group.
[j] Data were missing for 8 participants in Stroke group.
[k] Data were missing for 9 participants in HC group.
[l] Data were missing for 4 participants in PSD group.

were no significant differences in gender ($p = 0.756$) and age ($p = 0.121$), while significant differences were observed in blood systolic pressure ($p < 0.001$), blood diastolic pressure ($p < 0.001$), blood sugar level ($p < 0.001$), total cholesterol ($p < 0.01$), PHQ-9 scores ($p < 0.001$) and ADL scores ($p < 0.001$) among three groups. Stroke group and PSD group showed no significant differences in smoking ($p = 0.816$), drinking ($p = 0.230$), lesion hemisphere ($p = 0.582$), lesion size ($p = 0.992$). Compared with the Stroke group, the PSD patients exhibited significantly higher NIHSS scores ($p < 0.001$), SAS scores ($p < 0.001$), HAMD scores ($p < 0.001$) and CES-D scores ($p < 0.001$).

3.2. PSD-specific alterations in different ALFF metrics

In classic frequency band (0.01–0.08 Hz), significant among-group differences of ALFF-Classic were observed in bilateral middle frontal gyrus (MFG) and supplementary motor area (SMA), ipsilesional superior occipital gyrus (SOG), the triangular part of inferior frontal gyrus (IFGtriang) and the dorsolateral part of superior frontal gyrus (SFGdor), contralesional superior temporal gyrus (STG), insula (INS) and middle temporal gyrus (MTG) ($q < 0.05$, FDR corrected, cluster size > 20 voxels) (Table 2 and Fig. 2A). Post-hoc analyses (two-sample *t*-tests) revealed PSD-specific alterations in ALFF-Classic. That is, PSD group exhibited increased ALFF-Classic values in the bilateral MFG, ipsilesional SFGdor, contralesional INS and SMA when compared with both Stroke and HC groups ($p < 0.05$) (Table 2 and Fig. 3A).

In the slow-4 frequency band (0.027–0.073 Hz), there were significant differences in bilateral SFGdor and MFG, ipsilesional SOG, IFGtriang, median cingulate and paracingulate gyri (DCG) and SMA, contralesional INS, STG and MTG among three groups ($q < 0.05$, FDR corrected, cluster size > 20 voxels) (Table 2 and Fig. 2B). Post-hoc analyses (two-sample *t*-tests) showed increased ALFF in bilateral MFG, ipsilesional SFGdor and contralesional INS in PSD group relative to both Stroke and HC groups ($p < 0.05$). These brain regions reflected PSD-specific alterations in ALFF-Slow4 (Table 2 and Fig. 3B).

In the slow-5 frequency band (0.01–0.027 Hz), significant among-group differences were observed in bilateral hippocampus (HIP) and IFGtriang, ipsilesional middle occipital gyrus (MOG), SFGdor and the medial part of superior frontal gyrus (SFGmed), contralesional STG, MTG, rolandic operculum (ROL), INS, MFG, supramarginal gyrus (SMG), and precental gyrus (PreCG) ($q < 0.05$, FDR corrected, cluster size > 20 voxels) (Table 2 and Fig. 2C). PSD-specific alterations as revealed by post-hoc analyses (two-sample *t*-tests) characterized by increased ALFF-Slow5 in bilateral HIP, ipsilesional SFGmed, contralesional MFG, INS and ROL in PSD group when compared to both Stroke

Table 2
Among-group differences of ALFF in different frequency bands.

Brain region	Hemisphere	Voxel	F value	$p_{\text{uncorrected}}$ value	$q_{\text{FDR corrected}}$ value	MNI coordinate(mm)		
						x	y	z
Classic band (0.01–0.08 Hz)								
Superior occipital gyrus	IL	4089	23.847	5.75E-10	1.06E-05	−15	−87	12
Inferior frontal gyrus (triangular)	IL	26	16.973	1.65E-07	4.46E-05	−36	39	0
Superior temporal gyrus	CL	28	12.602	7.26E-06	3.85E-04	57	−18	0
Insula	CL	219	14.815	1.05E-06	1.23E-04	36	−3	18
Superior frontal gyrus (dorsolateral). I	IL	21	11.561	1.83E-05	6.76E-04	−21	51	6
Middle temporal gyrus	CL	121	20.376	9.61E-09	9.79E-06	57	−54	18
Superior frontal gyrus (dorsolateral)	IL	118	13.856	2.41E-06	1.98E-04	−12	39	36
Middle frontal gyrus	CL	71	18.272	5.52E-08	2.41E-05	30	9	36
Middle frontal gyrus	IL	41	10.086	6.87E-05	1.61E-03	−39	18	45
Supplementary motor area	IL	26	12.232	1.01E-05	4.72E-04	−3	18	51
Supplementary motor area	CL	20	7.876	5.17E-04	5.55E-03	12	24	54
Slow-4 (0.027–0.073 Hz)								
Insula	CL	233	14.215	1.77E-06	2.38E-04	36	−3	18
Superior occipital gyrus	IL	3577	24.057	4.86E-10	8.93E-06	−21	−78	27
Inferior frontal gyrus (triangular). I	IL	21	15.930	4.02E-07	1.01E-04	−36	39	0
Superior temporal gyrus	CL	23	11.634	1.71E-05	8.95E-04	57	−18	0
Middle temporal gyrus	CL	110	19.477	2.02E-08	2.47E-05	57	−54	18
Median cingulate and paracingulate gyri	IL	141	13.829	2.47E-06	2.93E-04	−12	−48	33
Inferior frontal gyrus (triangular)	IL	30	9.339	1.35E-04	3.05E-03	−51	21	27
Superior frontal gyrus (dorsolateral)	IL	82	12.878	5.69E-06	4.75E-04	−12	39	36
Middle frontal gyrus	CL	58	15.817	4.43E-07	1.08E-04	30	9	36
Middle frontal gyrus	IL	48	11.501	1.93E-05	9.56E-04	−39	18	45
Superior frontal gyrus (dorsolateral)	CL	22	8.585	2.69E-04	4.44E-03	21	30	48
Supplementary motor area	IL	22	10.999	3.02E-05	1.25E-03	−3	18	51
Slow-5 (0.01–0.027 Hz)								
Hippocampus	IL	98	13.702	2.76E-06	3.45E-04	−24	–33	0
Middle occipital gyrus	IL	2778	23.277	9.08E-10	1.67E-05	–33	−72	0
Hippocampus	CL	88	10.502	4.72E-05	1.72E-03	33	−24	−6
Superior temporal gyrus	CL	28	10.947	3.16E-05	1.36E-03	57	−18	0
Inferior frontal gyrus (triangular)	CL	62	10.437	5.01E-05	1.78E-03	39	36	0
Middle temporal gyrus	CL	37	14.842	1.03E-06	1.81E-04	57	−54	18
Rolandic operculum	CL	30	9.141	1.62E-04	3.67E-03	54	0	12
Insula	CL	30	11.278	2.35E-05	1.15E-03	33	−3	18
Rolandic operculum. S	CL	39	10.052	7.08E-05	2.21E-03	39	−18	24
Inferior frontal gyrus (triangular)	IL	23	7.619	6.56E-04	8.78E-03	−51	21	27
Middle frontal gyrus	CL	70	20.409	9.35E-09	2.14E-05	30	9	36
Superior frontal gyrus (medial)	IL	22	9.933	7.89E-05	2.36E-03	−12	39	33
Supramarginal gyrus	CL	40	11.165	2.60E-05	1.22E-03	60	−36	36
Superior frontal gyrus (dorsolateral)	IL	47	9.177	1.57E-04	3.60E-03	−18	21	51
Precental gyrus	CL	103	9.932	7.90E-05	2.36E-03	33	−15	54

Abbreviations: MNI, Montreal Neurological Institute; IL, ipsilesional hemisphere; CL, contralesional hemisphere; I, inferior; S, superior.

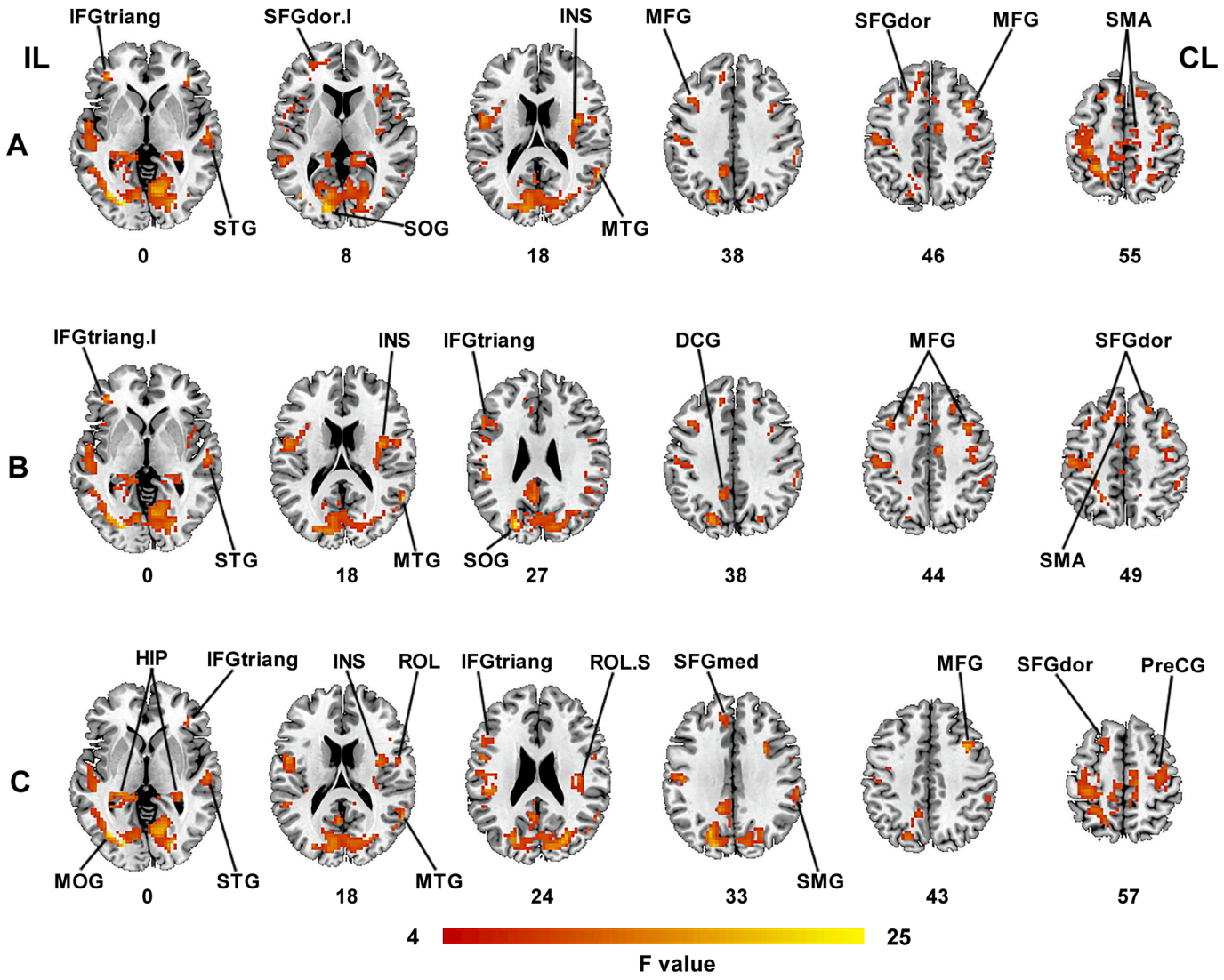

Fig. 2. Among-group differences of ALFF values in different frequency bands. There were significant differences of ALFF in (A) classic frequency band, (B) slow-4 frequency band, and (C) slow-5 frequency band (FDR correction at $q < 0.05$, cluster size > 20 voxels). ***Abbreviations:*** IL, ipsilesional hemisphere; CL, contralesional hemisphere; I, inferior; S, superior; IFGtriang, the triangular part of inferior frontal gyrus; STG, superior temporal gyrus; SFGdor, the dorsolateral part of superior frontal gyrus; SOG, superior occipital gyrus; INS, insula; MTG, middle temporal gyrus; MFG, middle frontal gyrus; SMA, supplementary motor area; DCG, median cingulate and paracingulate gyri; MOG, middle occipital gyrus; HIP, hippocampus; ROL, rolandic operculum; SFGmed, the medial part of superior frontal gyrus; SMG, supramarginal gyrus; PreCG, precental gyrus.

and HC groups ($p < 0.05$) (Table 2 and Fig. 3C).

For dynamic ALFF, there were no significant differences in dALFF-CV, while significant differences in dALFF-SD were observed in ipsilesional SMG and anterior cingulate gyri (ACG), contralesional HIP, SFGdor, angular gyrus (ANG), SFGmed and SMA among three groups ($q < 0.05$, FDR corrected, cluster size > 20 voxels) (Fig. 5A). Although Post-hoc analyses (two-sample *t*-tests) revealed no PSD-specific alterations of average dALFF-SD values in these regions, voxel-wise differences in dALFF-SD values were further inferred using two-sample *t*-test between Stroke and PSD groups within the mask obtained from ANOVA result. Compared to Stroke group, PSD showed decreased dALFF-SD in bilateral STG and postcentral gyrus (PoCG), ipsilesional cuneus (CUN), MTG, ROL, the opercular part of inferior frontal gyrus (IFGoperc), and MFG, contralesional INS, IFGtriang, DCG, and lingual gyrus (LING) (uncorrected $p < 0.05$, cluster size > 20 voxels) (Table 3 and Fig. 5B). 8-mm radius spherical ROIs centered on the peak coordinates of the between-group differences were then made to extract and compare dALFF-SD values between each pair of three groups. Results reflected the decreased dALFF-SD in contralesional STG in PSD group as compared with both Stroke and HC group ($p < 0.05$) (Table 3 and Fig. 5C). The dALFF results were validated by using the step size of 5 TR (Supplementary Fig. 1). Moreover, the among-group differences of ALFF remained largely unchanged when using mean FD as an additional covariate (Supplementary Fig. 2), and all PSD-specific alteration results of ALFF were largely unchanged by the comparisons between the PSD and Stroke groups after regressing out NIHSS scores (Supplementary Table 1).

3.3. Depression prediction in PSD

The average ALFF-Classic values in regions showing PSD-specific alterations could predict HAMD scores ($r = 0.458$, $p = 0.003$), but not PHQ-9 scores ($r = 0.200$, $p = 0.222$) and CES-D scores ($r = 0.147$, $p = 0.373$) in PSD group (Fig. 4A).

The average ALFF-Slow4 values extracted from the regions showing PSD-specific alterations could predict HAMD scores ($r = 0.470$, $p = 0.003$), not PHQ-9 scores ($r = 0.179$, $p = 0.274$) and CES-D scores ($r = 0.201$, $p = 0.220$) in PSD group (Fig. 4B).

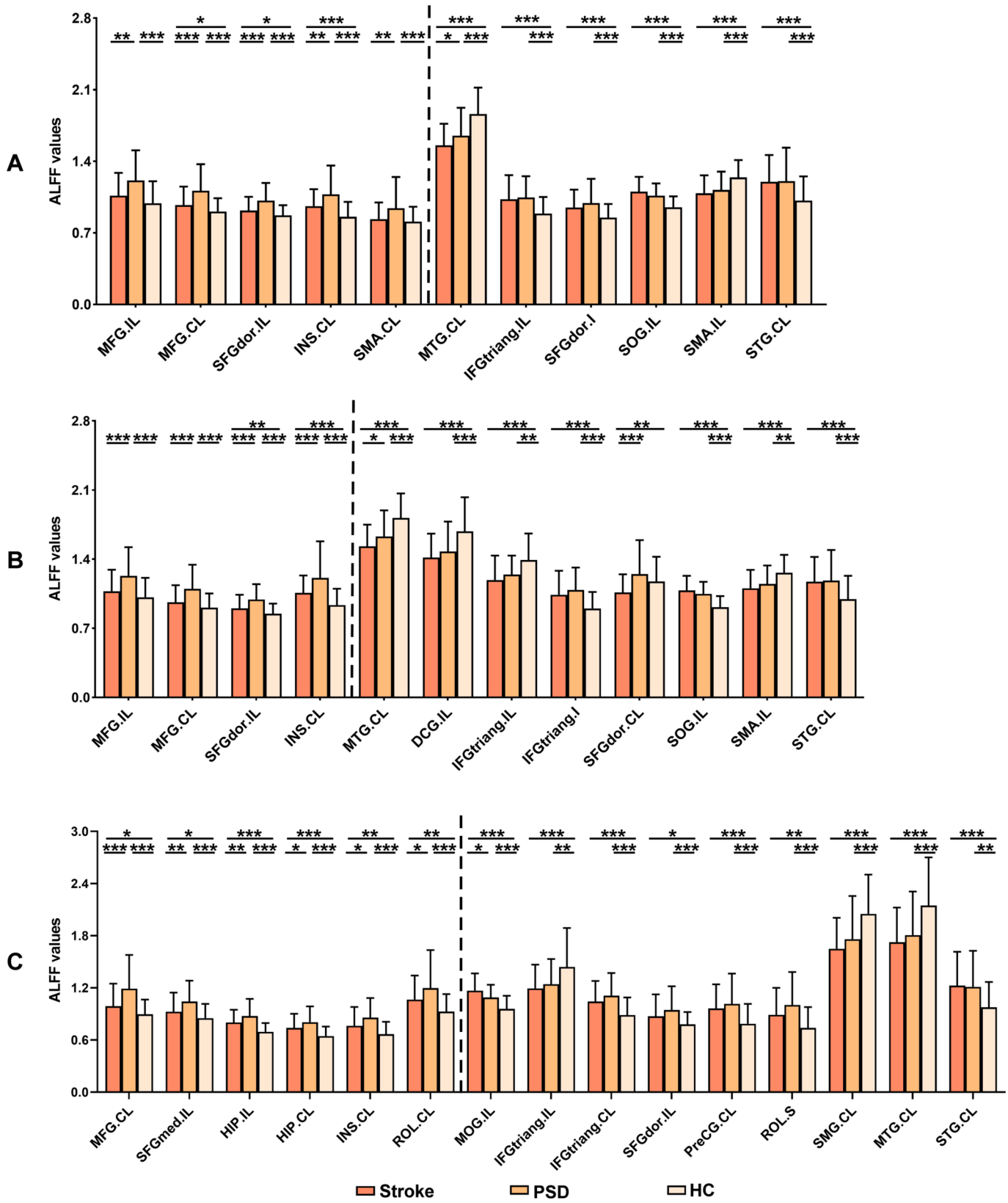

Fig. 3. Post-hoc comparisons of ALFF between each pair of three groups. Between-group differences of ALFF in (A) classic frequency band, (B) slow-4 frequency band, and (C) slow-5 frequency band. The regions on the left of dashed line showing PSD-specific alterations of ALFF. $^{*}p < 0.05$, $^{**}p < 0.01$, $^{***}p < 0.001$ ***Abbreviations:*** Stroke, stroke patients without depression; PSD, post-stroke depression; HC, healthy controls; IL, ipsilesional hemisphere; CL, contralesional hemisphere; I, inferior; S, superior; MFG, middle frontal gyrus; SFGdor, the dorsolateral part of superior frontal gyrus; INS, insula; SMA, supplementary motor area; MTG, middle temporal gyrus; IFGtriang, the triangular part of inferior frontal gyrus; SOG, superior occipital gyrus; STG, superior temporal gyrus; DCG, median cingulate and paracingulate gyri; SFGmed, the medial part of superior frontal gyrus; HIP, hippocampus; ROL, rolandic operculum; MOG, middle occipital gyrus; PreCG, precental gyrus; SMG, supramarginal gyrus.

Table 3
dALFF-SD differences between PSD and Stroke groups.

Brain region	Hemisphere	Voxel	T value	$p_{uncorrected}$ value	MNI coordinate(mm)		
					x	y	z
PSD < Stroke							
Cuneus	IL	237	−3.782	2.46E-04	−3	−66	24
Superior temporal gyrus	CL	26	−3.446	7.92E-04	45	−3	−15
Superior temporal gyrus	IL	71	−3.296	1.30E-03	−51	−6	0
Insula	CL	23	−3.972	1.24E-04	36	30	0
Middle temporal gyrus	IL	22	−3.272	1.40E-03	−57	−48	6
Rolandic operculum	IL	34	−2.605	1.04E-02	−48	−18	12
Inferior frontal gyrus (opercular)	IL	27	−4.020	1.04E-04	−48	15	15
Inferior frontal gyrus (triangular)	CL	36	−3.282	1.36E-03	36	18	24
Middle frontal gyrus	IL	62	−3.695	3.36E-04	−24	45	18
Inferior frontal gyrus (opercular part). S	IL	32	−2.992	3.38E-03	−45	3	24
Median cingulate and paracingulate gyri	CL	38	−3.431	8.33E-04	6	−30	33
Postcentral gyrus	CL	37	−2.796	6.05E-03	48	−15	39
Postcentral gyrus	IL	47	−3.061	2.74E-03	−24	−39	48
Lingual gyrus	CL	54	−3.336	1.14E-03	9	−63	−3

Abbreviations: MNI, Montreal Neurological Institute; PSD, post-stroke depression; Stroke, stroke patients without depression; IL, ipsilesional hemisphere; CL, contralesional hemisphere; S, superior.

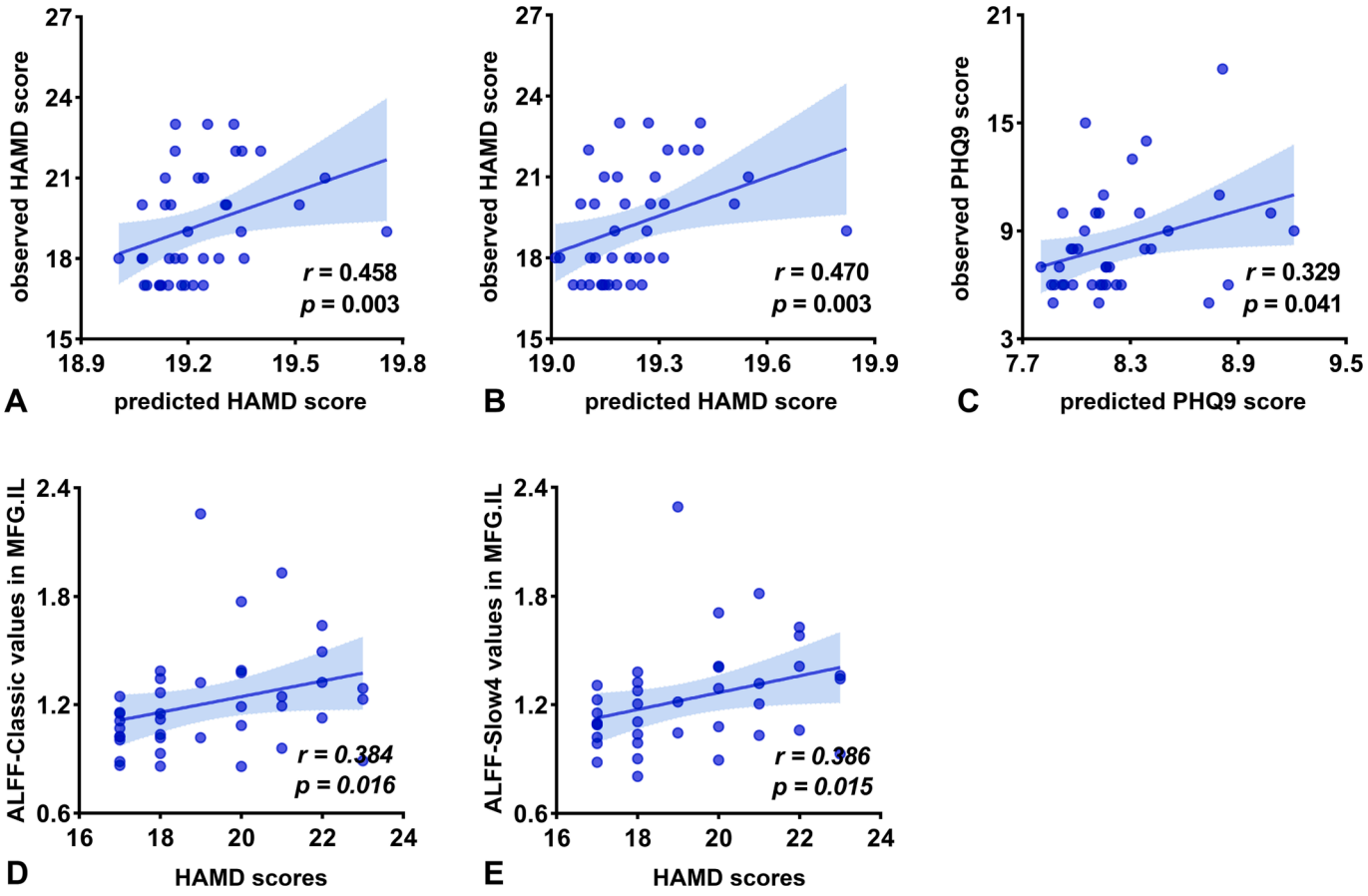

Fig. 4. Relationship between ALFF alterations and depression severity in PSD. Prediction of depression severity using the PSD-specific alterations of ALFF values in (A) classic frequency band, (B) slow-4 frequency band, and (C) slow-5 frequency band. Significant correlations were observed between HAMD scores and (D) the ALFF-Classic values and (E) ALFF-Slow4 values of ipsilesional MFG in PSD group. ***Abbreviations:*** HAMD, Hamilton Depression Rating Scale; PHQ-9, Patient Health Questionnaire-9; MFG, middle frontal gyrus; IL, ipsilesional hemisphere.

The average ALFF-Slow5 values of areas showing PSD-specific alterations could not predict CES-D scores ($r = 0.174$, $p = 0.290$) and HAMD scores ($r = 0.270$, $p = 0.096$), while could predict PHQ-9 scores ($r = 0.329$, $p = 0.041$) in PSD group (Fig. 4C).

3.4. Relationship between clinical characteristics and ALFF in PSD

ALFF-Classic ($r = 0.384$, $p = 0.016$) (Fig. 4D) and ALFF-Slow4 values ($r = 0.386$, $p = 0.015$) (Fig. 4E) of the ipsilesional MFG positively correlated with the HAMD scores in PSD patients. No significant correlations with depression severity and SAS were observed for any other ALFF metrics in regions showing PSD-specific alterations ($p > 0.05$)

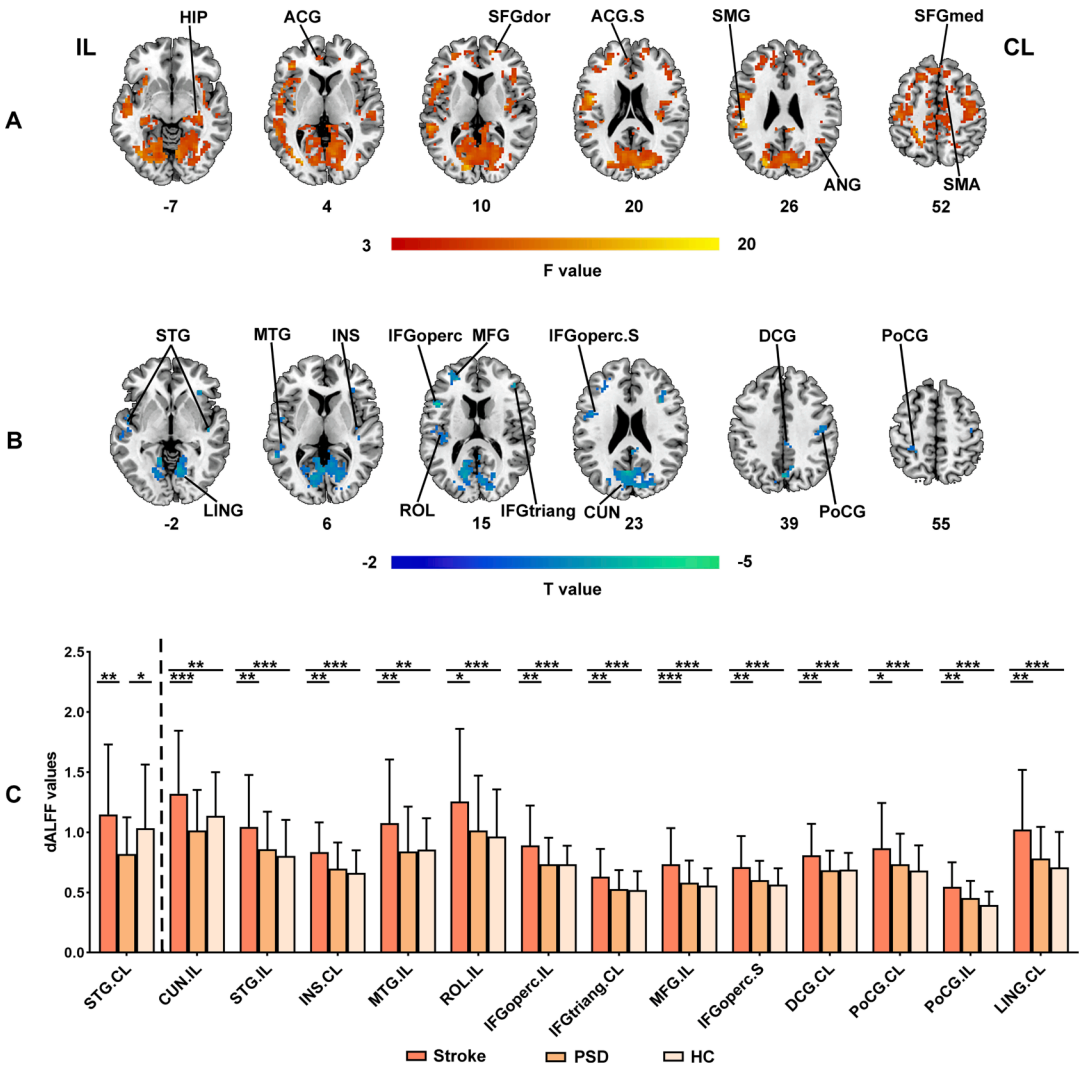

Fig. 5. Among group differences in dynamic ALFF. (A) dALFF-SD differences among Stroke, PSD and HC groups (FDR correction at $q < 0.05$, cluster size > 20 voxels). (B) dALFF-SD differences between Stroke and PSD groups (uncorrected $p < 0.05$, cluster size > 20 voxels). (C) Post-hoc comparisons of dALFF-SD between each pair of three groups. The regions on the left of dashed line showing PSD-specific alterations of dALFF-SD. $^{*}p < 0.05$, $^{**}p < 0.01$, $^{***}p < 0.001$. ***Abbreviations:*** Stroke, stroke patients without depression; PSD, post-stroke depression; HC, healthy controls; IL, ipsilesional hemisphere; CL, contralesional hemisphere; S, superior; HIP, hippocampus; ACG, anterior cingulate gyri; SFGdor, the dorsolateral part of superior frontal gyrus; SMG, supramarginal gyrus; ANG, angular gyrus; SFGmed, the medial part of superior frontal gyrus; SMA, supplementary motor area; STG, superior temporal gyrus; LING, lingual gyrus; MTG, middle temporal gyrus; INS, insula; IFGoperc, the opercular part of inferior frontal gyrus; ROL, rolandic operculum; MFG, middle frontal gyrus; IFGtriang, the triangular part of inferior frontal gyrus; CUN, cuneus; DCG, median cingulate and paracingulate gyri; PoCG, postcentral gyrus.

(Supplementary Table 2).

4. Discussion

The current study employed ALFF to investigate local functional abnormalities in PSD patients. We found the PSD-specific ALFF alterations were frequency-dependent and time-variant. Moreover, these frequency-dependent alterations could predict depression severity of PSD patients. Altogether, these findings demonstrate the emergence of local functional abnormalities in PSD patients and provide evidence for the complementary nature of different ALFF measures, which may help to elucidate the neural mechanisms underlying the PSD and may serve as the potential neuroimaging markers for early diagnosis and intervention of the disease.

4.1. PSD-specific ALFF alterations were frequency-dependent

Low-frequency oscillations of BOLD signals associated with spontaneous neural activity could be decomposed into different frequency bands, which were generated by distinct physiologic substrates and reflected different neural processes (Penttonen, 2003; Zuo et al., 2010). Among them, slow-4 and slow-5 mainly reflect the oscillations from gray matter signals (Zuo et al., 2010). The amplitude of the BOLD signals in these two frequency bands (i.e., ALFF-Slow4, ALFF-Slow5) were found to reveal distinct alterations in brain disorders, such as schizophrenia (Hare et al., 2017), Alzheimer's disease (Yang et al., 2020), and Parkinson's disease (Hou et al., 2014). In this study, we found that the PSD-specific alterations of ALFF exhibited different patterns in slow-4 and slow-5 frequency bands, suggesting frequency-dependent ALFF abnormalities in PSD.

PSD patients showed increased ALFF values in the bilateral middle frontal gyrus, the ipsilesional dorsolateral part of superior frontal gyrus, and the contralesional insula in both classic and slow-4 frequency bands. The results of the middle frontal gyrus and the dorsolateral part of superior frontal gyrus belong to the dorsolateral prefrontal cortex (DLPFC), which is a central component in the cognitive control network

(Sheline et al., 2010; Williams, 2016), and involved in attention control and cognitive and emotional information processing (Curtis and D'Esposito, 2003; Siegle et al., 2007; Wu et al., 2020b). It has been consistently reported that depression is associated with aberrant activity in DLPFC (Egorova et al., 2018; Fales et al., 2008; Galynker et al., 1998; Kerestes et al., 2012). For example, previous studies observed increased ALFF values in DLPFC in depression patients when compared to healthy controls (Liu et al., 2018; Liu et al., 2014). Regarding patients with brain lesions, Koenigs and colleagues found bilateral DLPFC lesions are correlated with higher levels of depression (Koenigs et al., 2008). In current study, bilateral DLPFC exhibited higher ALFF values in PSD patients. This is consistent with a previous study which also reported PSD-related increases of spontaneous activities in DLPFC (Egorova et al., 2017). Notably, the location of DLPFC from our results was overlapped with the center of the depression circuit as proposed by previous study, which found the DLPFC was more connected to lesions of PSD patients as compared to lesions of non-depressed stroke patients (Padmanabhan et al., 2019). Thus, we propose that increased activity in DLPFC may compensate for the lesions induced by stroke within the depression circuit in PSD. More importantly, ALFF-Slow4 and ALFF-Classic values in the ipsilesional DLPFC were positively correlated with HAMD scale in PSD patients. That is, the severer the depression of the patients, the higher the activity in DLPFC. All these findings together suggest that the abnormalities in DLPFC may have close relationship with the pathophysiological underpinnings in PSD and may serve as a promising treatment target for the disease.

As one component of the negative affect circuit, the insula is associated with the subjective feeling of emotions (Damasio et al., 2000; Williams, 2016). Previous studies frequently observed increased activation in insula when participants responded to negative emotional stimulus (Lane et al., 1997; McCabe et al., 2012; Perlman et al., 2012; Reiman et al., 1997). Our results of PSD-related increase of spontaneous neural activity in insula were also observed in patients with depression (Egorova et al., 2017; Liu et al., 2015; Liu et al., 2014). The results imply that the PSD and the primary depression not caused by focal brain lesions may share the similar neural underpinnings. It would be interesting for future studies to explore the similarities and differences between the depression patients caused by brain lesions and those not.

In addition, PSD-specific alterations of ALFF in contralesional supplementary motor area were only observed in classic frequency band. Despite generally being related to motor processing, accumulating MRI studies demonstrated that the supplementary motor area is also involved in emotional processing (Frodl et al., 2010a; Kozlowska et al., 2017; Wu et al., 2021). Given a considerable proportion of PSD patients accompanied by motor dysfunctions, we speculated that PSD-specific increase of ALFF-Classic in contralesional supplementary motor area may be related to the difficulties both in movement and emotion.

Whereas in slow-5 frequency band, PSD patients exhibited higher ALFF values in the bilateral hippocampus and the contralesional rolandic operculum except for similar results as in slow-4 frequency bands, i.e., bilateral DLPFC (contralesional middle frontal gyrus and ipsilesional medial part of superior frontal gyrus) and contralesional insula. The hippocampus is a vital part of the limbic system and mainly participated in the process of episodic memory and emotional regulation (Eichenbaum, 2013; Rive et al., 2013). Functional and structural abnormalities in hippocampus have been widely reported in depressed patients (Chen et al., 2017; Fairhall et al., 2010; Frodl et al., 2010b; Hamilton and Gotlib, 2008; MacMaster et al., 2008). Chen and colleagues found that patients with major depressive disorder exhibited higher ALFF in the bilateral hippocampus relative to the health controls (Chen et al., 2017). With respect to depression caused by stroke, we also observed increased activity in bilateral hippocampus in PSD. We speculate that the increased activity in hippocampus may be associated with cognitive impairments in PSD, which has been reported to be more severe as compared to nondepressed stroke patients (Kauhanen et al., 1999; Swardfager and MacIntosh, 2017). Future studies are required to testify the relationships between alterations of ALFF in hippocampus and cognitive dysfunction in PSD. The rolandic operculum is situated adjacent to the insula and participated in the awareness of interoceptive signals (Blefari et al., 2017), which in turn would influence emotional processing. Recent study has reported functional abnormalities in the left rolandic operculum in patients with recurrent depression (Sun et al., 2022). Sutoko and colleagues found that the degree of lesion in right rolandic operculum is associated with the severity of depression in PSD patients (Sutoko et al., 2020). Our results of higher ALFF values in the rolandic operculum in PSD further demonstrated that the deficits of rolandic operculum may contribute to the depression after stroke.

Of note, the regression analyses revealed that the PSD-specific alterations of ALFF in different frequency bands could predict the depression severity in patients. Both the alterations of ALFF-Classic and ALFF-Slow4 could predict HAMD scores, while that of ALFF-Slow5 could predict PHQ-9 scores. The signals of different frequency bands are linked to different neural processes such as cognitive functions including emotional regulation and attention (Knyazev, 2007; Zuo et al., 2010). Our results provide further evidence for frequency-dependent property of BOLD signals and indicate the ALFF in different frequency bands hold the abilities to capture the alterations of neural activity from different aspects, and thus reflect the PSD-specific changes in complementary ways.

4.2. *PSD-specific ALFF alterations were time-variant*

Dynamic characteristics of intrinsic brain activity have been reported to link with cognitive adaption, brain development, and brain disorders such as depression (Cui et al., 2020). In current study, we found the PSD-specific dynamic alterations of ALFF (i.e., decreased dALFF-SD) in contralesional superior temporal gyrus. The superior temporal gyrus is involved in emotional and social cognitive processing (Adolphs, 2003; Gallagher and Frith, 2003; Takahashi et al., 2010), and found to be abnormal in depressed patients (Fitzgerald et al., 2008). Thus, the decreased dALFF in contralesional superior temporal gyrus might be related to cognitive deficits in PSD, a speculation could be tested in future. Notably, there was no correlation between the dALFF in contralesional superior temporal gyrus and depression scales in PSD group. Therefore, the reproductivity and reliability of temporal variability of BOLD signal in PSD should be further examined in future study.

5. Limitations

The present study has several limitations. First, our study was a cross-sectional design that the patients were recruited within 1 month after stroke onset, thus fail to investigate the abnormal patterns of neural activity as disease progress. Future longitudinal studies are required to explore the alterations of ALFF in PSD in different phases after stroke. Second, the group-differences in dALFF did not pass multiple comparison correction. Therefore, these findings of dALFF should be considered with caution and need to be validated with the larger sample size of PSD patients. Third, at present, the clinical treatments for PSD patients were similar to MDD, such as taking antidepressants or rTMS treatment targeted on the left DLPFC. The specific treatment for PSD could be developed If we could identify the PSD-related brain alterations as compared to depressed non-stroke patients in the future. Fourth, no supporting information was provided though all the stroke patients stated they did not have leukoaraiosis before stroke onset. Future studies collecting T2WI and FLAIR image for patients when they were admitted to the hospital could give the information of the leukoaraiosis. Fifth, we failed to assess the cognitive performance in the patients, and thus cannot explore the association between the alterations of ALFF in hippocampus and cognitive dysfunction in PSD. Future studies using Mini-Mental State Examination scale or Montreal Cognitive Assessment in patients can help clarify this issue. Finally, the depression severity of PSD patients in our study was within the range of mild to moderately

severe depression (PHQ-9) or moderate depression (HAMD). Our prediction results need to be further validated in PSD patients with different depression severity in future study, especially for those in severe depression category.

6. Conclusion

The current study demonstrated that the local functional alterations in PSD patients were frequency-dependent and time-variant, which may help to elucidate the neural mechanisms underlying the PSD and may serve as the potential neuroimaging markers for early diagnosis and intervention of the disease. Our results also suggest the necessity of applying both ALFF in different frequency bands and dynamic ALFF for characterizing the local functions in health and brain disorders.

CRediT authorship contribution statement

Xiumei Wu: Conceptualization, Methodology, Data curation, Formal analysis, Investigation, Writing – original draft, Writing – review & editing, Visualization. **Luoyu Wang:** Conceptualization, Methodology, Data curation, Formal analysis, Investigation, Writing – original draft, Writing – review & editing, Visualization. **Haibo Jiang:** Investigation, Writing – review & editing. **Yanhui Fu:** Investigation, Writing – review & editing. **Tiantian Wang:** Investigation, Writing – review & editing. **Zhenqiang Ma:** Investigation, Writing – review & editing. **Xiaoyan Wu:** Investigation, Writing – review & editing. **Yiying Wang:** Investigation, Writing – review & editing. **Fengmei Fan:** Conceptualization, Investigation, Validation, Writing – original draft, Writing – review & editing. **Yulin Song:** Conceptualization, Investigation, Validation, Writing – original draft, Writing – review & editing. **Yating Lv:** Conceptualization, Methodology, Investigation, Validation, Writing – original draft, Writing – review & editing.

Declaration of Competing Interest

The authors declare that they have no known competing financial interests or personal relationships that could have appeared to influence the work reported in this paper.

Data availability

Data will be made available on request.

Acknowledgments

We thank all the patients and volunteers for participating in this study. This work was supported by the National Key R&D Program of China (No. 2017YFC1310000), Zhejiang Provincial Natural Science Foundation of China (No. LGJ22H180001), Zhejiang Medical and Health Science and Technology Project (No. 2021KY249) and the Hangzhou Normal University (No. 2022HSDYJSKY295).

Data availability statement

According to the privacy protection policy of the Center for Cognition and Brain Disorders, Hangzhou Normal University, all data that support the findings of this study is not available in open access. However, researchers who are interested in accessing data could contact the corresponding author, who will help contact the committee of the center for data requisition.

Appendix A. Supplementary data

Supplementary data to this article can be found online at https://doi.org/10.1016/j.nicl.2023.103445.

References

Adolphs, R., 2003. Cognitive neuroscience of human social behaviour. Nat. Rev. Neurosci. 4, 165–178. https://doi.org/10.1038/nrn1056.

Allen, E.A., Damaraju, E., Plis, S.M., Erhardt, E.B., Eichele, T., Calhoun, V.D., 2014. Tracking whole-brain connectivity dynamics in the resting state. Cereb. Cortex 24, 663–676. https://doi.org/10.1093/cercor/bhs352.

Allman, C., Amadi, U., Winkler, A.M., Wilkins, L., Filippini, N., Kischka, U., Stagg, C.J., Johansen-Berg, H., 2016. Ipsilesional anodal tDCS enhances the functional benefits of rehabilitation in patients after stroke. Sci. Transl. Med. 8 https://doi.org/10.1126/scitranslmed.aad5651.

Ayerbe, L., Ayis, S., Wolfe, C.D., Rudd, A.G., 2013. Natural history, predictors and outcomes of depression after stroke: systematic review and meta-analysis. Br. J. Psychiatry 202, 14–21. https://doi.org/10.1192/bjp.bp.111.107664.

Balaev, V., Orlov, I., Petrushevsky, A., Martynova, O., 2018. Functional connectivity between salience, default mode and frontoparietal networks in post-stroke depression. J. Affect. Disord. 227, 554–562. https://doi.org/10.1016/j.jad.2017.11.044.

Bestmann, S., Swayne, O., Blankenburg, F., Ruff, C.C., Teo, J., Weiskopf, N., Driver, J., Rothwell, J.C., Ward, N.S., 2010. The role of contralesional dorsal premotor cortex after stroke as studied with concurrent TMS-fMRI. J. Neurosci. 30, 11926–11937. https://doi.org/10.1523/JNEUROSCI.5642-09.2010.

Blefari, M.L., Martuzzi, R., Salomon, R., Bello-Ruiz, J., Herbelin, B., Serino, A., Blanke, O., Foxe, J., 2017. Bilateral Rolandic operculum processing underlying heartbeat awareness reflects changes in bodily self-consciousness. Eur. J. Neurosci. 45 (10), 1300–1312.

Bu, X., Hu, X., Zhang, L., Li, B., Zhou, M., Lu, L., Hu, X., Li, H., Yang, Y., Tang, W., Gong, Q., Huang, X., 2019. Investigating the predictive value of different resting-state functional MRI parameters in obsessive-compulsive disorder. Transl. Psychiatry 9, 17. https://doi.org/10.1038/s41398-018-0362-9.

Cai, W., Mueller, C., Li, Y.J., Shen, W.D., Stewart, R., 2019. Post stroke depression and risk of stroke recurrence and mortality: A systematic review and meta-analysis. Ageing Res. Rev. 50, 102–109. https://doi.org/10.1016/j.arr.2019.01.013.

Chang, M., Edmiston, E.K., Womer, F.Y., Zhou, Q., Wei, S., Jiang, X., Zhou, Y., Ye, Y., Huang, H., Zuo, X.N., Xu, K., Tang, Y., Wang, F., 2019. Spontaneous low-frequency fluctuations in the neural system for emotional perception in major psychiatric disorders: amplitude similarities and differences across frequency bands. J. Psychiatry Neurosci. 44, 132–141. https://doi.org/10.1503/jpn.170226.

Chen, V.C., Shen, C.Y., Liang, S.H., Li, Z.H., Hsieh, M.H., Tyan, Y.S., Lu, M.L., Lee, Y., McIntyre, R.S., Weng, J.C., 2017. Assessment of brain functional connectome alternations and correlation with depression and anxiety in major depressive disorders. PeerJ 5, e3147.

Cui, Q., Sheng, W., Chen, Y., Pang, Y., Lu, F., Tang, Q., Han, S., Shen, Q., Wang, Y., Xie, A., Huang, J., Li, D., Lei, T., He, Z., Chen, H., 2020. Dynamic changes of amplitude of low-frequency fluctuations in patients with generalized anxiety disorder. Hum. Brain Mapp. 41, 1667–1676. https://doi.org/10.1002/hbm.24902.

Curtis, C.E., D'Esposito, M., 2003. Persistent activity in the prefrontal cortex during working memory. Trends Cogn. Sci. 7, 415–423. https://doi.org/10.1016/s1364-6613(03)00197-9.

Damasio, A., Grabowski, T., Bechara, A., Damasio, H., Ponto, L., Parvizi, J., Hichwa, R., 2000. Subcortical and Cortical Brain Activity During the Feeling of Self-Generated Emotions. Nat. Neurosci. 3, 1049–1056. https://doi.org/10.1038/79871.

Egorova, N., Veldsman, M., Cumming, T., Brodtmann, A., 2017. Fractional amplitude of low-frequency fluctuations (fALFF) in post-stroke depression. Neuroimage Clin. 16, 116–124. https://doi.org/10.1016/j.nicl.2017.07.014.

Egorova, N., Cumming, T., Shirbin, C., Veldsman, M., Werden, E., Brodtmann, A., 2018. Lower cognitive control network connectivity in stroke participants with depressive features. Transl. Psychiatry 7, 4. https://doi.org/10.1038/s41398-017-0038-x.

Eichenbaum, H., 2013. Hippocampus: remembering the choices. Neuron 77, 999–1001. https://doi.org/10.1016/j.neuron.2013.02.034.

Fairhall, S.L., Sharma, S., Magnusson, J., Murphy, B., 2010. Memory related dysregulation of hippocampal function in major depressive disorder. Biol. Psychol. 85, 499–503. https://doi.org/10.1016/j.biopsycho.2010.09.002.

Fales, C.L., Barch, D.M., Rundle, M.M., Mintun, M.A., Snyder, A.Z., Cohen, J.D., Mathews, J., Sheline, Y.I., 2008. Altered emotional interference processing in affective and cognitive-control brain circuitry in major depression. Biol. Psychiatry 63, 377–384. https://doi.org/10.1016/j.biopsych.2007.06.012.

Fitzgerald, P.B., Laird, A.R., Maller, J., Daskalakis, Z.J., 2008. A meta-analytic study of changes in brain activation in depression. Hum. Brain Mapp. 29, 683–695. https://doi.org/10.1002/hbm.20426.

Fox, M.D., Greicius, M., 2010. Clinical applications of resting state functional connectivity. Front. Syst. Neurosci. 4, 19. https://doi.org/10.3389/fnsys.2010.00019.

Fox, M.D., Raichle, M.E., 2007. Spontaneous fluctuations in brain activity observed with functional magnetic resonance imaging. Nat. Rev. Neurosci. 8, 700–711. https://doi.org/10.1038/nrn2201.

Friston, K.J., Williams, S., Howard, R., Frackowiak, R.S.J., Turner, R., 1996. Movement-Related effects in fMRI time-series. Magn. Reson. Med. 35, 346–355. https://doi.org/10.1002/mrm.1910350312.

Frodl, T., Bokde, A.L.W., Scheuerecker, J., Lisiecka, D., Schoepf, V., Hampel, H., Möller, H.-J., Brückmann, H., Wiesmann, M., Meisenzahl, E., 2010a. Functional Connectivity Bias of the Orbitofrontal Cortex in Drug-Free Patients with Major Depression. Biol. Psychiatry 67, 161–167. https://doi.org/10.1016/j.biopsych.2009.08.022.

Frodl, T., Reinhold, E., Koutsouleris, N., Donohoe, G., Bondy, B., Reiser, M., Moller, H.J., Meisenzahl, E.M., 2010b. Childhood stress, serotonin transporter gene and brain

structures in major depression. Neuropsychopharmacology 35, 1383–1390. https://doi.org/10.1038/npp.2010.8.
Fu, Z.N., Tu, Y.H., Di, X., Du, Y.H., Pearlson, G.D., Turner, J.A., Biswal, B.B., Zhang, Z.G., Calhoun, V.D., 2018. Characterizing dynamic amplitude of low-frequency fluctuation and its relationship with dynamic functional connectivity: An application to schizophrenia. Neuroimage 180, 619–631. https://doi.org/10.1016/j.neuroimage.2017.09.035.
Gallagher, H.L., Frith, C.D., 2003. Functional imaging of 'theory of mind'. Trends Cogn. Sci. 7, 77–83. https://doi.org/10.1016/s1364-6613(02)00025-6.
Galynker, I., Cai, J., Ongseng, F., Finestone, H., Dutta, E., Serseni, D., 1998. Hypofrontality and negative symptoms in major depressive disorder. J. Nucl. Med.: Off. Publ. Soc. Nucl. Med. 39, 608–612.
Goodin, P., Lamp, G., Vidyasagar, R., Connelly, A., Rose, S., Campbell, B.C.V., Tse, T., Ma, H., Howells, D., Hankey, G.J., Davis, S., Donnan, G., Carey, L.M., 2019. Correlated Resting-State Functional MRI Activity of Frontostriatal, Thalamic, Temporal, and Cerebellar Brain Regions Differentiates Stroke Survivors with High Compared to Low Depressive Symptom Scores. Neural Plast. 2019, 2357107. https://doi.org/10.1155/2019/2357107.
Guo, J., Biswal, B.B., Han, S., Li, J., Yang, S., Yang, M., Chen, H., 2019. Altered dynamics of brain segregation and integration in poststroke aphasia. Hum. Brain Mapp. 40, 3398–3409. https://doi.org/10.1002/hbm.24605.
Hackett, M.L., Pickles, K., 2014. Part I: frequency of depression after stroke: an updated systematic review and meta-analysis of observational studies. Int. J. Stroke 9, 1017–1025. https://doi.org/10.1111/ijs.12357.
Hamilton, J.P., Gotlib, I.H., 2008. Neural substrates of increased memory sensitivity for negative stimuli in major depression. Biol. Psychiatry 63, 1155–1162. https://doi.org/10.1016/j.biopsych.2007.12.015.
Hare, S.M., Ford, J.M., Ahmadi, A., Damaraju, E., Belger, A., Bustillo, J., Lee, H.J., Mathalon, D.H., Mueller, B.A., Preda, A., van Erp, T.G., Potkin, S.G., Calhoun, V.D., Turner, J.A., Functional Imaging Biomedical Informatics Research, N., 2017. Modality-Dependent Impact of Hallucinations on Low-Frequency Fluctuations in Schizophrenia. Schizophr Bull. 43, 389-396. https://doi.org/10.1093/schbul/sbw093.
Hou, Y., Wu, X., Hallett, M., Chan, P., Wu, T., 2014. Frequency-dependent neural activity in Parkinson's disease. Hum. Brain Mapp. 35, 5815–5833. https://doi.org/10.1002/hbm.22587.
Hutchison, R.M., Womelsdorf, T., Allen, E.A., Bandettini, P.A., Calhoun, V.D., Corbetta, M., Della Penna, S., Duyn, J.H., Glover, G.H., Gonzalez-Castillo, J., Handwerker, D.A., Keilholz, S., Kiviniemi, V., Leopold, D.A., de Pasquale, F., Sporns, O., Walter, M., Chang, C., 2013. Dynamic functional connectivity: promise, issues, and interpretations. Neuroimage 80, 360–378. https://doi.org/10.1016/j.neuroimage.2013.05.079.
Jia, X.-Z., Wang, J., Sun, H.-Y., Zhang, H., Liao, W., Wang, Z., Yan, C.-G., Song, X.-W., Zang, Y.-F., 2019. RESTplus: an improved toolkit for resting-state functional magnetic resonance imaging data processing. Science Bulletin. 64, 953–954. https://doi.org/10.1016/j.scib.2019.05.008.
Kauhanen, M., Korpelainen, J.T., Hiltunen, P., Brusin, E., Mononen, H., Maatta, R., Nieminen, P., Sotaniemi, K.A., Myllyla, V.V., 1999. Poststroke depression correlates with cognitive impairment and neurological deficits. Stroke 30, 1875–1880. https://doi.org/10.1161/01.STR.30.9.1875.
Kerestes, R., Bhagwagar, Z., Nathan, P.J., Meda, S.A., Ladouceur, C.D., Maloney, K., Matuskey, D., Ruf, B., Saricicek, A., Wang, F., Pearlson, G.D., Phillips, M.L., Blumberg, H.P., 2012. Prefrontal cortical response to emotional faces in individuals with major depressive disorder in remission. Psychiatry Res. 202, 30–37. https://doi.org/10.1016/j.pscychresns.2011.11.004.
Knyazev, G.G., 2007. Motivation, emotion, and their inhibitory control mirrored in brain oscillations. Neurosci. Biobehav. Rev. 31, 377–395. https://doi.org/10.1016/j.neubiorev.2006.10.004.
Koenigs, M., Huey, E.D., Calamia, M., Raymont, V., Tranel, D., Grafman, J., 2008. Distinct regions of prefrontal cortex mediate resistance and vulnerability to depression. J. Neurosci. 28, 12341–12348. https://doi.org/10.1523/JNEUROSCI.2324-08.2008.
Kozlowska, K., Griffiths, K.R., Foster, S.L., Linton, J., Williams, L.M., Korgaonkar, M.S., 2017. Grey matter abnormalities in children and adolescents with functional neurological symptom disorder. Neuroimage Clin. 15, 306–314. https://doi.org/10.1016/j.nicl.2017.04.028.
Lane, R.D., Reiman, E.M., Ahern, G.L., Schwartz, G.E., Davidson, R.J., 1997. Neuroanatomical correlates of happiness, sadness, and disgust. Am. J. Psychiatry 154, 926–933.
Leonardi, N., Van De Ville, D., 2015. On spurious and real fluctuations of dynamic functional connectivity during rest. Neuroimage 104, 430–436. https://doi.org/10.1016/j.neuroimage.2014.09.007.
Li, J., Duan, X., Cui, Q., Chen, H., Liao, W., 2019. More than just statics: temporal dynamics of intrinsic brain activity predicts the suicidal ideation in depressed patients. Psychol. Med. 49, 852–860. https://doi.org/10.1017/S0033291718001502.
Liang, Y., Yao, Y.C., Zhao, L., Shi, L., Chen, Y.K., Mok, V.C., Ungvari, G.S., Chu, W.C., Tang, W.K., 2020. Topological reorganization of the default mode network in patients with poststroke depressive symptoms: A resting-state fMRI study. J. Affect. Disord. 260, 557–568. https://doi.org/10.1016/j.jad.2019.09.051.
Liao, W., Li, J., Ji, G.J., Wu, G.R., Long, Z., Xu, Q., Duan, X., Cui, Q., Biswal, B.B., Chen, H., 2019. Endless Fluctuations: Temporal Dynamics of the Amplitude of Low Frequency Fluctuations. IEEE Trans. Med. Imaging 38, 2523–2532. https://doi.org/10.1109/TMI.2019.2904555.
Liu, C.H., Ma, X., Song, L.P., Fan, J., Wang, W.D., Lv, X.Y., Zhang, Y., Li, F., Wang, L., Wang, C.Y., 2015. Abnormal spontaneous neural activity in the anterior insular and anterior cingulate cortices in anxious depression. Behav. Brain Res. 281, 339–347. https://doi.org/10.1016/j.bbr.2014.11.047.
Liu, C.H., Guo, J., Lu, S.L., Tang, L.R., Fan, J., Wang, C.Y., Wang, L., Liu, Q.Q., Liu, C.Z., 2018. Increased Salience Network Activity in Patients With Insomnia Complaints in Major Depressive Disorder. Front. Psych. 9, 93. https://doi.org/10.3389/fpsyt.2018.00093.
Liu, J., Ren, L., Womer, F.Y., Wang, J., Fan, G., Jiang, W., Blumberg, H.P., Tang, Y., Xu, K., Wang, F., 2014. Alterations in amplitude of low frequency fluctuation in treatment-naive major depressive disorder measured with resting-state fMRI. Hum. Brain Mapp. 35, 4979–4988. https://doi.org/10.1002/hbm.22526.
Loubinoux, I., Kronenberg, G., Endres, M., Schumann-Bard, P., Freret, T., Filipkowski, R. K., Kaczmarek, L., Popa-Wagner, A., 2012. Post-stroke depression: mechanisms, translation and therapy. J. Cell Mol. Med. 16, 1961–1969. https://doi.org/10.1111/j.1582-4934.2012.01555.x.
Lv, Y., Margulies, D.S., Cameron Craddock, R., Long, X., Winter, B., Gierhake, D., Endres, M., Villringer, K., Fiebach, J., Villringer, A., 2013. Identifying the perfusion deficit in acute stroke with resting-state functional magnetic resonance imaging. Ann. Neurol. 73, 136–140. https://doi.org/10.1002/ana.23763.
MacMaster, F.P., Mirza, Y., Szeszko, P.R., Kmiecik, L.E., Easter, P.C., Taormina, S.P., Lynch, M., Rose, M., Moore, G.J., Rosenberg, D.R., 2008. Amygdala and hippocampal volumes in familial early onset major depressive disorder. Biol. Psychiatry 63, 385–390. https://doi.org/10.1016/j.biopsych.2007.05.005.
McCabe, C., Woffindale, C., Harmer, C.J., Cowen, P.J., 2012. Neural Processing of Reward and Punishment in Young People at Increased Familial Risk of Depression. Biol. Psychiatry 72, 588–594. https://doi.org/10.1016/j.biopsych.2012.04.034.
Murphy, K., Fox, M.D., 2017. Towards a consensus regarding global signal regression for resting state functional connectivity MRI. Neuroimage 154, 169–173. https://doi.org/10.1016/j.neuroimage.2016.11.052.
Nachev, P., Coulthard, E., Jäger, H.R., Kennard, C., Husain, M., 2008. Enantiomorphic normalization of focally lesioned brains. Neuroimage 39, 1215–1226. https://doi.org/10.1016/j.neuroimage.2007.10.002.
Padmanabhan, J.L., Cooke, D., Joutsa, J., Siddiqi, S.H., Ferguson, M., Darby, R.R., Soussand, L., Horn, A., Kim, N.Y., Voss, J.L., Naidech, A.M., Brodtmann, A., Egorova, N., Gozzi, S., Phan, T.G., Corbetta, M., Grafman, J., Fox, M.D., 2019. A Human Depression Circuit Derived From Focal Brain Lesions. Biol. Psychiatry 86, 749–758. https://doi.org/10.1016/j.biopsych.2019.07.023.
Penttonen, M., 2003. Natural logarithmic relationship between brain oscillators. Thalamus Relat. Syst. 2, 145–152. https://doi.org/10.1016/s1472-9288(03)00007-4.
Perlman, G., Simmons, A.N., Wu, J., Hahn, K.S., Tapert, S.F., Max, J.E., Paulus, M.P., Brown, G.G., Frank, G.K., Campbell-Sills, L., Yang, T.T., 2012. Amygdala response and functional connectivity during emotion regulation: a study of 14 depressed adolescents. J. Affect. Disord. 139, 75–84. https://doi.org/10.1016/j.jad.2012.01.044.
Power, J.D., Barnes, K.A., Snyder, A.Z., Schlaggar, B.L., Petersen, S.E., 2012. Spurious but systematic correlations in functional connectivity MRI networks arise from subject motion. Neuroimage 59, 2142–2154. https://doi.org/10.1016/j.neuroimage.2011.10.018.
Quan, X., Hu, S.u., Meng, C., Cheng, L., Lu, Y., Xia, Y., Li, W., Liang, H., Li, M., Liang, Z., Zheng, Y.u., 2022. Frequency-Specific Changes of Amplitude of Low-Frequency Fluctuations in Patients with Acute Basal Ganglia Ischemic Stroke. Neural Plast. 2022, 1–10.
Reiman, E.M., Lane, R.D., Ahern, G.L., Schwartz, G.E., Davidson, R.J., Friston, K.J., Yun, L.S., Chen, K., 1997. Neuroanatomical correlates of externally and internally generated human emotion. Am. J. Psychiatry 154, 918–925.
Rive, M.M., van Rooijen, G., Veltman, D.J., Phillips, M.L., Schene, A.H., Ruhe, H.G., 2013. Neural correlates of dysfunctional emotion regulation in major depressive disorder. A systematic review of neuroimaging studies. Neurosci. Biobehav. Rev. 37, 2529–2553. https://doi.org/10.1016/j.neubiorev.2013.07.018.
Robinson, R.G., Jorge, R.E., 2016. Post-Stroke Depression: A Review. Am. J. Psychiatry 173, 221–231. https://doi.org/10.1176/appi.ajp.2015.15030363.
Rorden, C., Bonilha, L., Fridriksson, J., Bender, B., Karnath, H.O., 2012. Age-specific CT and MRI templates for spatial normalization. Neuroimage 61, 957–965. https://doi.org/10.1016/j.neuroimage.2012.03.020.
Schaechter, J.D., Fricker, Z.P., Perdue, K.L., Helmer, K.G., Vangel, M.G., Greve, D.N., Makris, N., 2009. Microstructural status of ipsilesional and contralesional corticospinal tract correlates with motor skill in chronic stroke patients. Hum. Brain Mapp. 30, 3461–3474. https://doi.org/10.1002/hbm.20770.
Sheline, Y.I., Price, J.L., Yan, Z., Mintun, M.A., 2010. Resting-state functional MRI in depression unmasks increased connectivity between networks via the dorsal nexus. PNAS 107, 11020–11025. https://doi.org/10.1073/pnas.1000446107.
Shi, Y., Zeng, Y., Wu, L., Liu, W., Liu, Z., Zhang, S., Yang, J., Wu, W., 2017. A Study of the Brain Abnormalities of Post-Stroke Depression in Frontal Lobe Lesion. Sci. Rep. 7, 13203. https://doi.org/10.1038/s41598-017-13681-w.
Siegle, G.J., Thompson, W., Carter, C.S., Steinhauer, S.R., Thase, M.E., 2007. Increased amygdala and decreased dorsolateral prefrontal BOLD responses in unipolar depression: related and independent features. Biol. Psychiatry 61, 198–209. https://doi.org/10.1016/j.biopsych.2006.05.048.
Skidmore, F.M., Yang, M., Baxter, L., von Deneen, K., Collingwood, J., He, G., Tandon, R., Korenkevych, D., Savenkov, A., Heilman, K.M., Gold, M., Liu, Y., 2013. Apathy, depression, and motor symptoms have distinct and separable resting activity patterns in idiopathic Parkinson disease. Neuroimage 81, 484–495. https://doi.org/10.1016/j.neuroimage.2011.07.012.
Smith, S.M., Miller, K.L., Moeller, S., Xu, J., Auerbach, E.J., Woolrich, M.W., Beckmann, C.F., Jenkinson, M., Andersson, J., Glasser, M.F., Van Essen, D.C., Feinberg, D.A., Yacoub, E.S., Ugurbil, K., 2012. Temporally-independent functional

modes of spontaneous brain activity. PNAS 109, 3131–3136. https://doi.org/10.1073/pnas.1121329109.
Sun, J.F., Chen, L.M., He, J.K., Wang, Z., Guo, C.L., Ma, Y., Luo, Y., Gao, D.Q., Hong, Y., Fang, J.L., Xu, F.Q., 2022. A Comparative Study of Regional Homogeneity of Resting-State fMRI Between the Early-Onset and Late-Onset Recurrent Depression in Adults. Front. Psychol. 13, 849847 https://doi.org/10.3389/fpsyg.2022.849847.
Sutoko, S., Atsumori, H., Obata, A., Funane, T., Kandori, A., Shimonaga, K., Hama, S., Yamawaki, S., Tsuji, T., 2020. Lesions in the right Rolandic operculum are associated with self-rating affective and apathetic depressive symptoms for post-stroke patients. Sci. Rep. 10, 20264. https://doi.org/10.1038/s41598-020-77136-5.
Swardfager, W., MacIntosh, B.J., 2017. Depression, Type 2 Diabetes, and Poststroke Cognitive Impairment. Neurorehabil. Neural Repair 31, 48–55. https://doi.org/10.1177/1545968316656054.
Takahashi, T., Yucel, M., Lorenzetti, V., Walterfang, M., Kawasaki, Y., Whittle, S., Suzuki, M., Pantelis, C., Allen, N.B., 2010. An MRI study of the superior temporal subregions in patients with current and past major depression. Prog Neuropsychopharmacol Biol Psychiatry. 34, 98–103. https://doi.org/10.1016/j.pnpbp.2009.10.005.
Veldsman, M., Cumming, T., Brodtmann, A., 2015. Beyond BOLD: optimizing functional imaging in stroke populations. Hum. Brain Mapp. 36, 1620–1636. https://doi.org/10.1002/hbm.22711.
Wang, L., Kong, Q., Li, K., Su, Y., Zeng, Y., Zhang, Q., Dai, W., Xia, M., Wang, G., Jin, Z., Yu, X., Si, T., 2016. Frequency-dependent changes in amplitude of low-frequency oscillations in depression: A resting-state fMRI study. Neurosci. Lett. 614, 105–111. https://doi.org/10.1016/j.neulet.2016.01.012.
Wang, P., Li, R., Liu, B., Wang, C., Huang, Z., Dai, R., Song, B., Yuan, X., Yu, J., Li, J., 2019. Altered Static and Temporal Dynamic Amplitude of Low-Frequency Fluctuations in the Background Network During Working Memory States in Mild Cognitive Impairment. Front. Aging Neurosci. 11, 152. https://doi.org/10.3389/fnagi.2019.00152.
Wijeratne, T., Sales, C., 2021. Understanding Why Post-Stroke Depression May Be the Norm Rather Than the Exception: The Anatomical and Neuroinflammatory Correlates of Post-Stroke Depression. J. Clin. Med. 10 (8), 1674.
Williams, L.M., 2016. Precision psychiatry: a neural circuit taxonomy for depression and anxiety. Lancet Psychiatry 3, 472–480. https://doi.org/10.1016/s2215-0366(15)00579-9.
Wu, Z., Luo, Q., Wu, H., Wu, Z., Zheng, Y., Yang, Y., He, J., Ding, Y., Yu, R., Peng, H., 2020a. Amplitude of Low-Frequency Oscillations in Major Depressive Disorder With Childhood Trauma. Front. Psych. 11, 596337 https://doi.org/10.3389/fpsyt.2020.596337.
Wu, Z., Luo, Y., Gao, Y.u., Han, Y., Wu, K., Li, X., 2020b. The Role of Frontal and Occipital Cortices in Processing Sustained Visual Attention in Young Adults with Attention-Deficit/Hyperactivity Disorder: A Functional Near-Infrared Spectroscopy Study. Neurosci. Bull. 36 (6), 659–663.
Wu, P., Zhang, A., Sun, N., Lei, L., Liu, P., Wang, Y., Li, H., Yang, C., Zhang, K., 2021. Cortical Thickness Predicts Response Following 2 Weeks of SSRI Regimen in First-Episode, Drug-Naive Major Depressive Disorder: An MRI Study. Front. Psych. 12, 751756 https://doi.org/10.3389/fpsyt.2021.751756.
Yan, C.G., Wang, X.D., Zuo, X.N., Zang, Y.F., 2016. DPABI: Data Processing & Analysis for (Resting-State) Brain Imaging. Neuroinformatics 14, 339–351. https://doi.org/10.1007/s12021-016-9299-4.
Yan, C.G., Yang, Z., Colcombe, S.J., Zuo, X.N., Milham, M.P., 2017. Concordance among indices of intrinsic brain function: Insights from inter-individual variation and temporal dynamics. Sci Bull (Beijing). 62, 1572–1584. https://doi.org/10.1016/j.scib.2017.09.015.
Yang, L., Yan, Y., Li, Y., Hu, X., Lu, J., Chan, P., Yan, T., Han, Y., 2020. Frequency-dependent changes in fractional amplitude of low-frequency oscillations in Alzheimer's disease: a resting-state fMRI study. Brain Imaging Behav. 14, 2187–2201. https://doi.org/10.1007/s11682-019-00169-6.
Zang, Y.F., He, Y., Zhu, C.Z., Cao, Q.J., Sui, M.Q., Liang, M., Tian, L.X., Jiang, T.Z., Wang, Y.F., 2007. Altered baseline brain activity in children with ADHD revealed by resting-state functional MRI. Brain Dev. 29, 83–91. https://doi.org/10.1016/j.braindev.2006.07.002.
Zhang, P., Xu, Q., Dai, J., Wang, J., Zhang, N., Luo, Y., 2014. Dysfunction of affective network in post ischemic stroke depression: a resting-state functional magnetic resonance imaging study. Biomed. Res. Int. 2014, 846830. https://doi.org/10.1155/2014/846830.
Zhang, X.F., He, X., Wu, L., Liu, C.J., Wu, W., 2019. Altered Functional Connectivity of Amygdala with the Fronto-Limbic-Striatal Circuit in Temporal Lobe Lesion as a Proposed Mechanism for Poststroke Depression. Am. J. Phys. Med. Rehabil. 98, 303–310. https://doi.org/10.1097/PHM.0000000000001081.
Zhang, P., Wang, J., Xu, Q., Song, Z., Dai, J., Wang, J., 2018. Altered functional connectivity in post-ischemic stroke depression: A resting-state functional magnetic resonance imaging study. Eur. J. Radiol. 100, 156–165. https://doi.org/10.1016/j.ejrad.2018.01.003.
Zuo, X.N., Di Martino, A., Kelly, C., Shehzad, Z.E., Gee, D.G., Klein, D.F., Castellanos, F. X., Biswal, B.B., Milham, M.P., 2010. The oscillating brain: complex and reliable. Neuroimage 49, 1432–1445. https://doi.org/10.1016/j.neuroimage.2009.09.037.